Supporting Figures

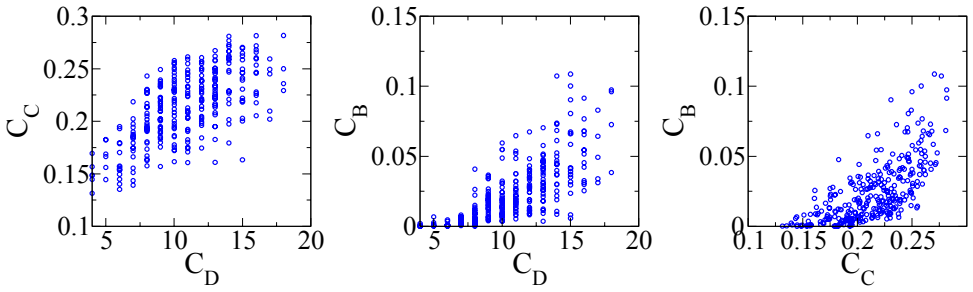

Figure S1. Scatter plots of (A) C_C vs C_D, (B) C_B vs C_D, and (C) C_C vs C_B.

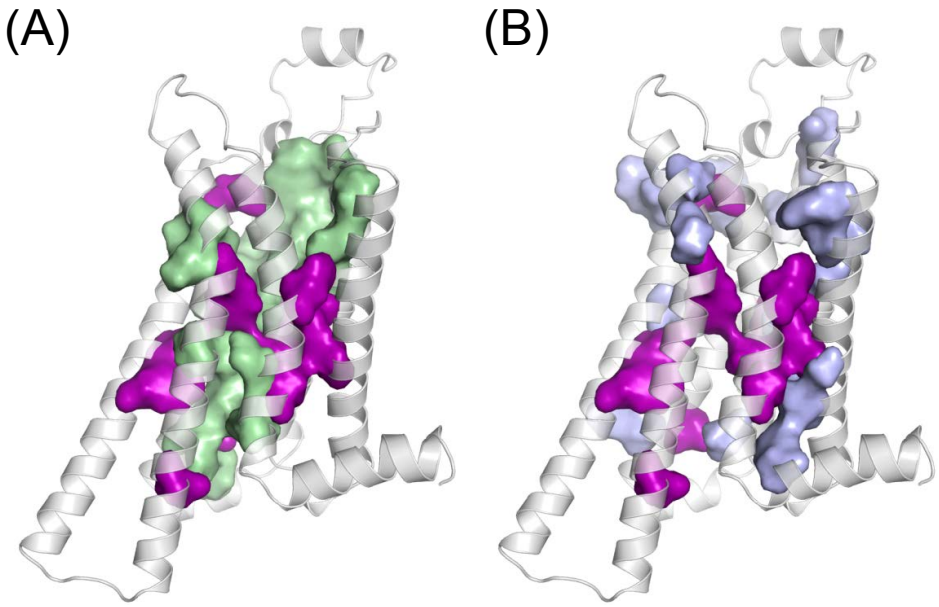

Figure S2. Residues with (A) $C_B(\geq 0.05)$ (group I and II in Fig.2C) and with (B) $\Delta G/k_BT(\geq 1.5)$ in AR family (group I and III in Fig.2C)

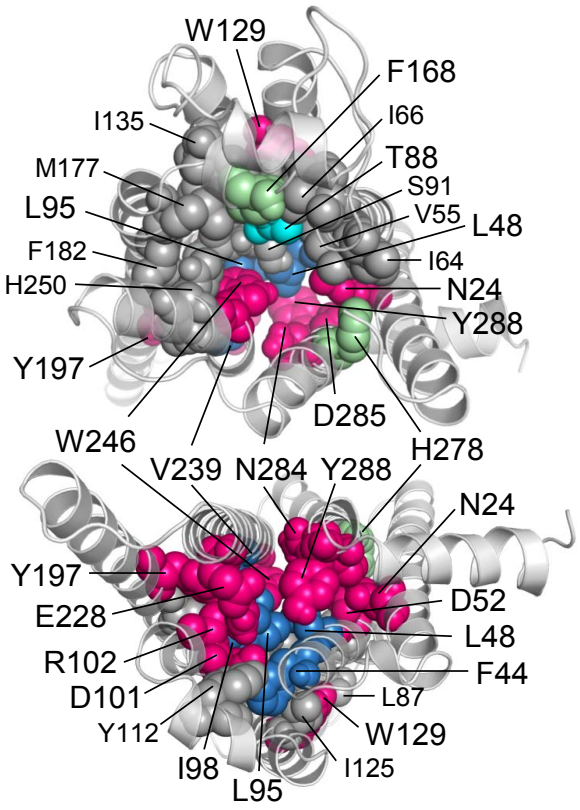

Figure S3. The residues with $C_B \geq 0.05$ represented by spheres in the extracellular view (top) and intracellular view (top). The color indices are same as in the Figure 2D.

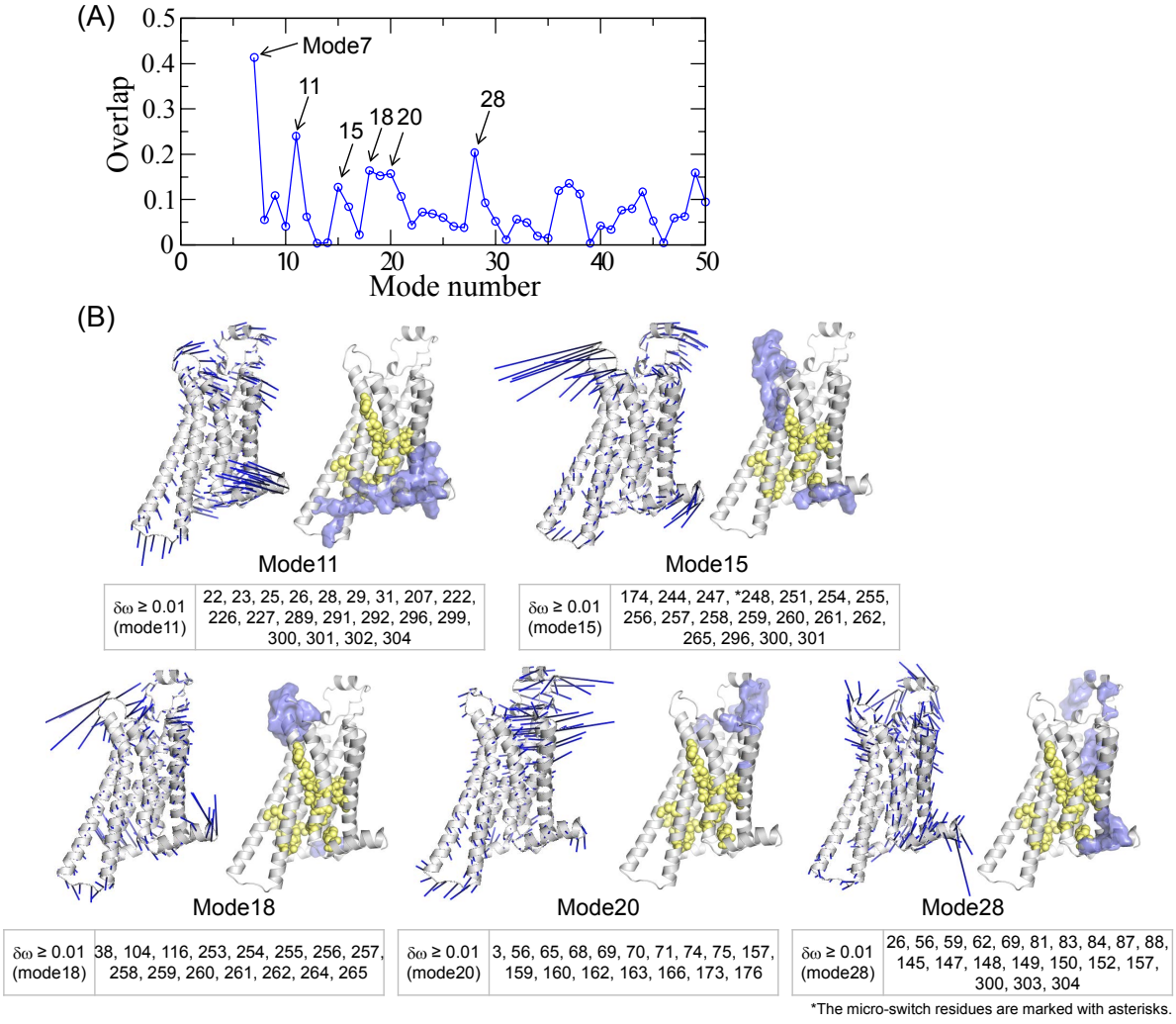

δω ≥ 0.01 (mode11)	22, 23, 25, 26, 28, 29, 31, 207, 222, 226, 227, 289, 291, 292, 296, 299, 300, 301, 302, 304

δω ≥ 0.01 (mode15)	174, 244, 247, *248, 251, 254, 255, 256, 257, 258, 259, 260, 261, 262, 265, 296, 300, 301

δω ≥ 0.01 (mode18)	38, 104, 116, 253, 254, 255, 256, 257, 258, 259, 260, 261, 262, 264, 265

δω ≥ 0.01 (mode20)	3, 56, 65, 68, 69, 70, 71, 74, 75, 157, 159, 160, 162, 163, 166, 173, 176

δω ≥ 0.01 (mode28)	26, 56, 59, 62, 69, 81, 83, 84, 87, 88, 145, 147, 148, 149, 150, 152, 157, 300, 303, 304

*The micro-switch residues are marked with asterisks.

Figure S4. (A) The degree of overlap, $\cos(\vec{r}_{apo\to ago} \cdot \vec{v}_M)$, calculated between the conformational change from apo to agonist-bound state and normal mode M of apo form (B) Residues with high $\delta\omega$ values for several normal modes of the apo form ($M = 11$, 15, 18, 20, 28). The residues with $\delta\omega \geq 0.01$ are represented with light-blue surfaces, and their residue numbers are listed below. For comparison, the locations of the micro-switch residues are depicted using yellow spheres.

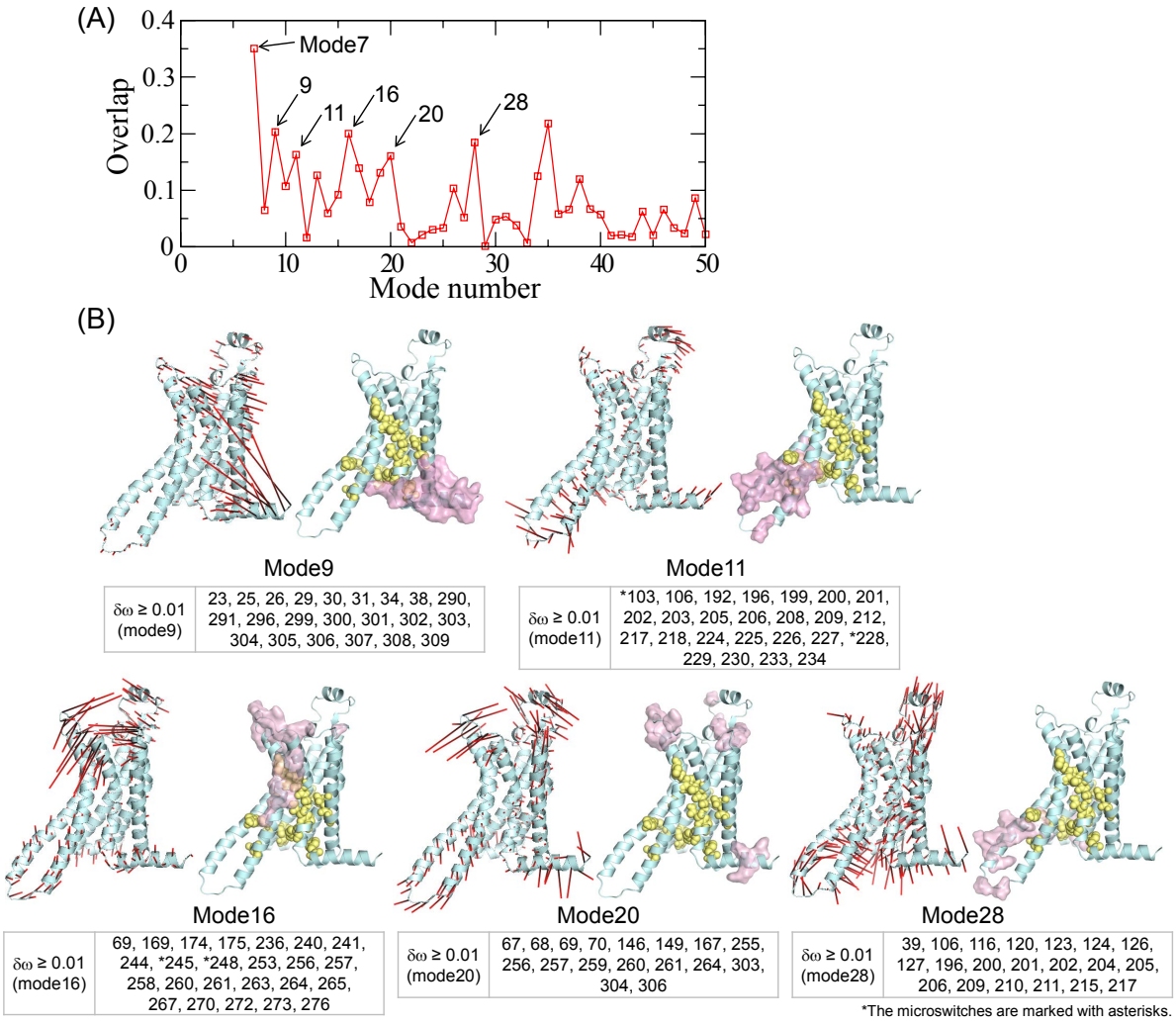

Figure S5. (A) The degree of overlap, $\cos(\vec{r}_{apo\to ago} \cdot \vec{v}_M)$, calculated between the conformational change from apo to agonist-bound state and normal mode M of agonist-bound form (B) Residues with high $\delta\omega$ values for several normal modes of the agonist-bound form ($M = 9$, 11, 16, 20, 28). The residues with $\delta\omega \geq 0.01$ are represented with pink surfaces, and their residue numbers are listed below. For comparison, the locations of the micro-switch residues are depicted using yellow spheres.

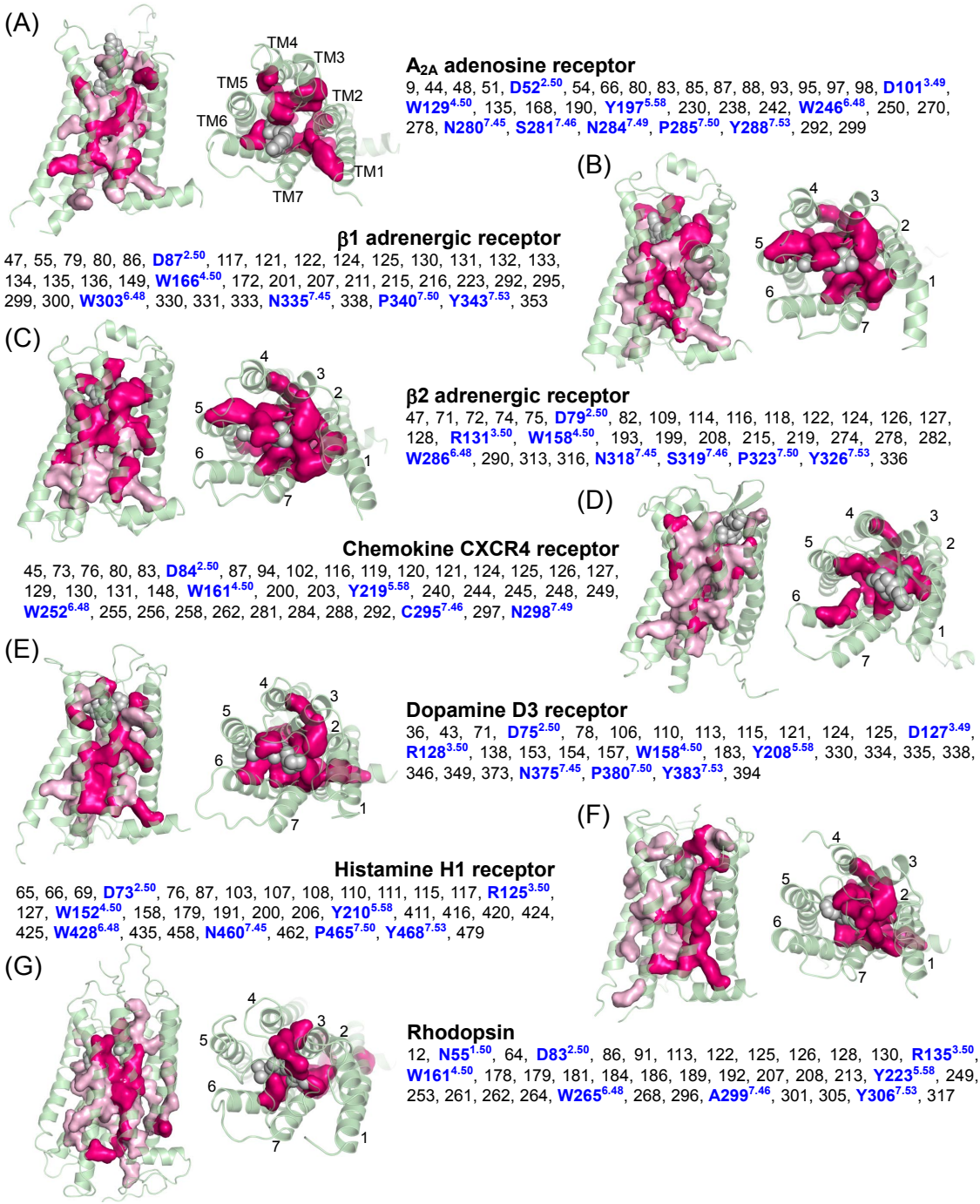

Figure S6. Network of residues with $C_B \geq 0.05$ represented in pink and $C_B \geq 0.075$ in magenta for the proteins belonging to the class A GPCR family. The residue networks are depicted using surfaces, and the residue indices are listed. Shown are the side and extracellular (top) views of GPCRs with the bound ligands displayed in gray spheres. The PDB IDs used in the calculations are as follows: A_{2A} adenosine receptor (3EML), $\beta 1$ adrenergic receptor (2VT4), $\beta 2$ adrenergic receptor (3NYA), Chemokine CXCR4 receptor (3ODU), Dopamine D3 receptor (3PBL), Histamine H1 receptor (3RZE), Rhodopsin (1U19).

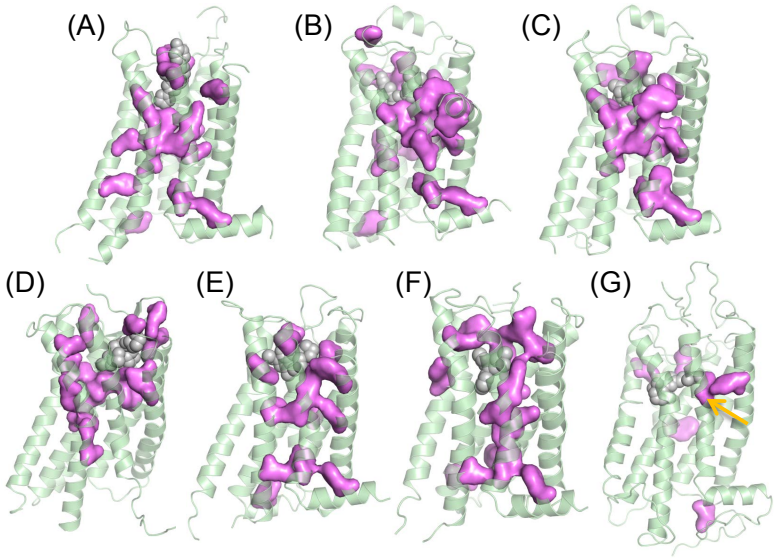

Receptor	TM1	TM2	ECL1	TM3	ICL2	TM4	ECL2	TM5	TM6	TM7	helix8
A_{2A} adenosine	9	*52		87,93, 95	112	*129,135, 139	168,169	190,*197	242,*246, 250	270,278, *280,*288	299
β1 adrenergic	47,48, 55	*87		117,122, 130,132	149	*166	201	207	*303	317,330, 333,*335, 338,*343	353
β2 adrenergic	47	*79,82		109,114, 124		*158	193	199	282,*286, 290	313,316, *318,*323, *326	336
Chemokine CXCR4	32,45	87, 94	102	116,120, 124			183,190	200,203	244,248, 256,262		
Dopamine D3	36,43			106,110	138	*158	183		330,338, 346	365,373, *375,*383	394
Histamine H1		65, 69, *73		103,108, 110,127			179	191,200	416,435	458,*460, *468	479
Rhodopsin	43,67					*161	178	203		296	

*The microswitch residues are marked with asterisks.

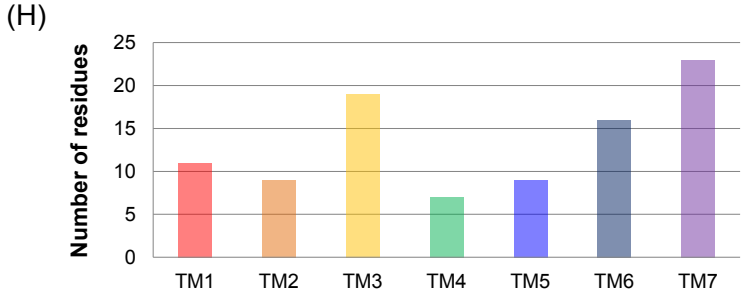

Figure S7. Glycine scanning (network vulnerability) analysis of the crystallized class A GPCRs. (A) A_{2A} adenosine receptor (PDB ID: 3EML). (B) Adrenergic $\beta 1$ receptor (2VT4). (C) Adrenergic $\beta 2$ receptor (3NYA). (D) Chemokine CXCR4 receptor (3ODU). (E) Dopamine D3 receptor (3PBL). (F) Histamine H1 receptor (3RZE). (G) Rhodopsin (1U19). The residues with high network vulnerability ($|\Gamma| \geq 0.003$) are depicted using pink surfaces. The bound ligands are shown in gray spheres. The list of residues with $|\Gamma| \geq 0.003$ are given in the table. (H) Total number of the highly vulnerable residues in each TM.

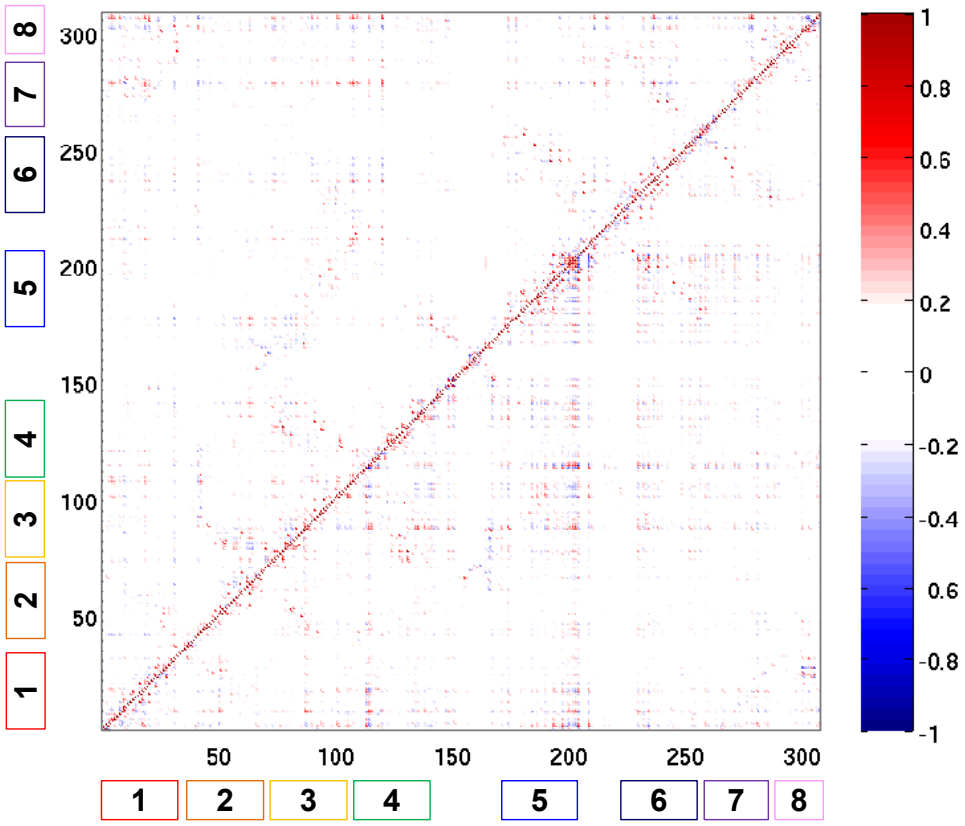

Figure S8. Cross-correlation map of the residue centralities during the 300 nsec MD simulation in the apo form (the upper left panel) and the agonist-bound form (the lower right panel).

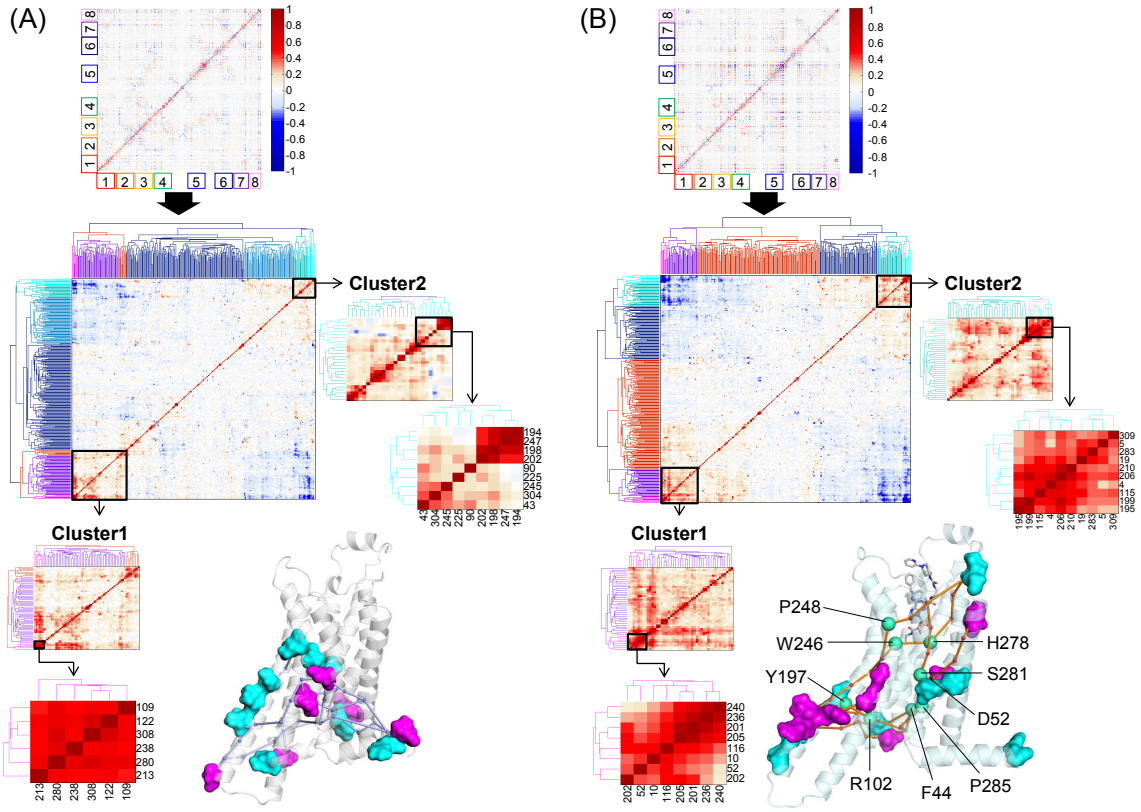

Figure S9. Clusters of long-range cross-correlated residues calculated for A_{2A}AR. (A) Cross-correlation map calculated for the apo form using Eq. 2 and its hierarchical clustering analysis. Highly cross-correlated clusters are enclosed with black boxes (cluster1 and cluster2). In the clusters, cross-correlated residue pairs with $CC_{ij} \geq 0.5$ are represented using cyan and magenta surfaces for the cluster1 and cluster2, respectively. Cross-correlated residue pairs are linked with minimal paths. (B) Same calculations for the agonist-bound form.

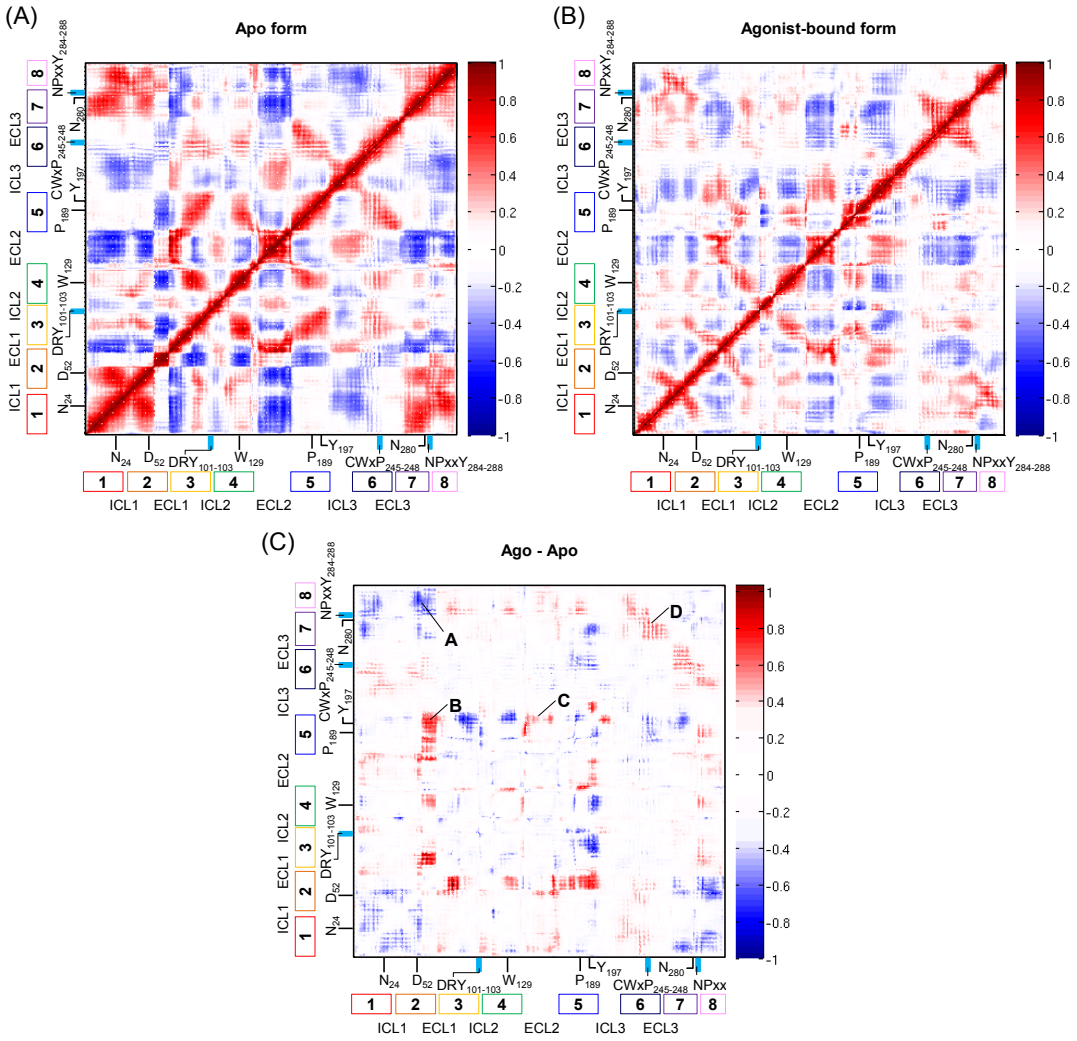

Figure S10. Cross-correlations of fluctuations for (A) apo, (B) agonist-bound forms, and (C) their difference calculated with MD trajectories. TM regions (TM1-TM7 and helix 8), intracellular loops (ICLs), extracellular loops (ECLs), and important structural motifs including microswitches are marked. The difference map in (C) shows that there is a dynamic coupling between extracellular ligand binding site and intracellular G-protein binding site: An agonist binding increases the correlation between the extracellular part of TM2 and the intracellular part of TM5 (region marked with "B" in (C)); whereas reduces the correlation of the extracellular part of TM2 and TM7-helix 8 (region "A"). In addition, the cross-correlation between the extracellular ligand binding site and intracellular G-protein binding site ("C" and "D" regions) is increased.

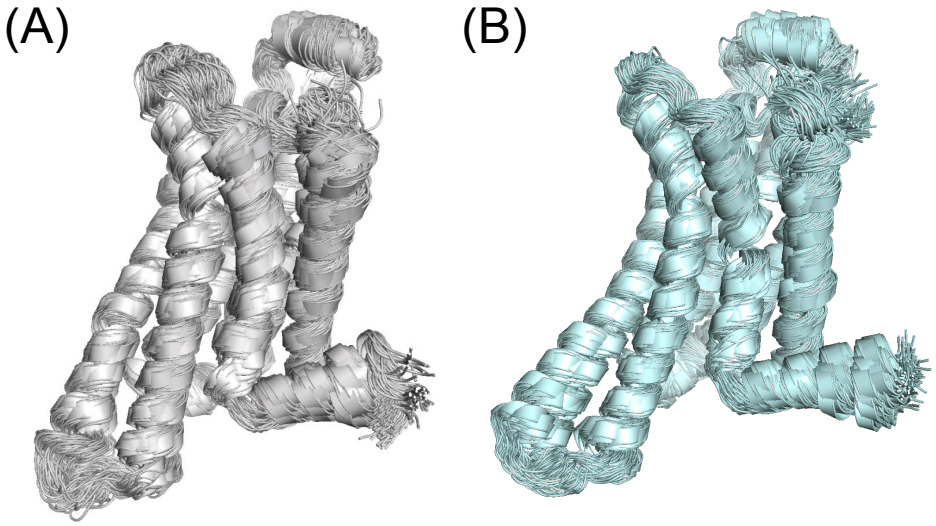

Figure S11. Ensemble of structures obtained from MD simulations for the (A) apo and (B) agonist-bound form.